Pergamon

Tetrahedron Vol. 51, No. 15, pp. 4255-4276, 1995

0040-4020/95 $9.50+0.00

0040-4020(94)01117-6

Mechanism and Regiochemistry of Azametallacyclobutene Formation from Imidozirconocene Complexes and Alkynes

Sun Yeoul Lee and Robert G. Bergman*

Department of Chemistry, University of California, Berkeley, CA 94720-1460

Abstract. This paper reports kinetic and regiochemistry studies that bear on the mechanism of overall [2 + 2] cycloaddition of alkynes with the imidozirconium complexes $Cp_2(L)Zr{=}NR$ (1; R = 2,6-$Me_2C_6H_3$ or *t*-Bu; L = 4-*tert*-butylpyridine or $OPPh_3$) to give heterometallacycles of type 2 (Scheme I). The kinetics are consistent with a dissociative mechanism (Path A in Scheme I) in which a rapid equilibrium involving reversible loss of a dative ligand (L) and generation of the transient intermediate $Cp_2Zr{=}NR$ is followed by reaction of this intermediate with the alkyne. Measurement of the relative rates of reaction of $Cp_2Zr{=}NR$ with 3-hexyne and di-*p*-tolylacetylene, and studies of the cycloaddition regioselectivity observed with unsymmetrically *p*-substituted diarylacetylenes, provided information about steric and electronic effects on the cycloaddition. These experiments support a conclusion that the reaction of the intermediate imido complex with alkynes proceeds via a four-center transition state having little charge separation. Under thermodynamic conditions, product distributions appear to be influenced predominantly by the ability of the group on the α-carbon to stabilize the metallacycle 2 by delocalization of partial negative charge.

INTRODUCTION

Although mononuclear group 4 imido complexes are rare and typically display a lack of reactivity,[1,2] the metal nitrogen multiple bonds of imidozirconocene complexes, $Cp_2(L)Zr{=}NR$ (e.g. R = 2,6-$Me_2C_6H_3$ or CMe_3, L = THF) (1), recently synthesized in our group, have shown unique reactivity toward organic substrates. These zirconium compounds activate C-H and N-H bonds and undergo overall 2+2 cycloaddition reactions with alkynes, some alkenes, and imines.[3-7] The alkyne cycloadditions lead to zirconocene azametallacyclobutenes in high yield (eq 1).[4,5] There are only a

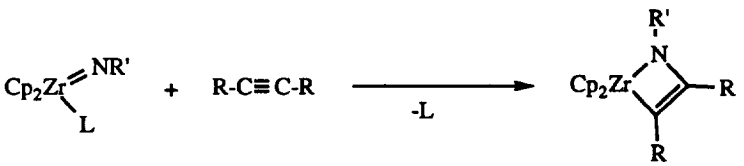

(1)

few examples of other metallacycles[8-11] generated from 2+2 cycloaddition between alkynes and metal nitrogen multiply-bonded complexes, although cycloadditions of alkylidenes with alkynes have been studied[12-14] and these metallacycles have been proposed as intermediates in the polymerization of acetylenes.[15-18] Therefore, we decided to examine the mechanism of the 2+2 cycloaddition of

$Cp_2Zr(NR)(L)$ (R = 2,6-$Me_2C_6H_3$, CMe_3; L = $OPPh_3$, 4-*tert*-butylpyridine) with diphenylacetylene and substituted diarylacetylenes.

RESULTS

Kinetics of azametallacyclobutene formation. Two possible pathways for the formation of azametallacyclobutene from the cycloaddition reaction of **1** with an alkyne are illustrated in Scheme I. The first (Path A) involves direct attack of an alkyne on **1** followed by (or simultaneous with)

Scheme I

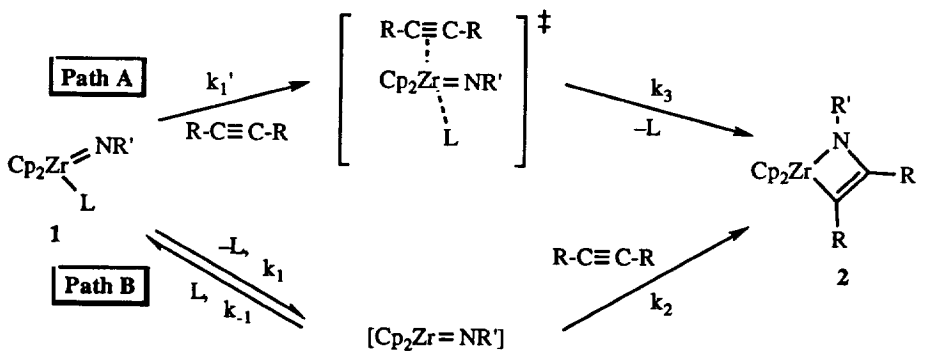

1a; R' = 2,6-$Me_2C_6H_3$, L = THF
1b; R' = 2,6,-$Me_2C_6H_3$, L = 4-*tert*-butylpyridine
1c; R' = CMe_3, L = $OPPh_3$

2a; R' = 2,6-$Me_2C_6H_3$, R = *p*-$CH_3C_6H_4$
2b; R' = 2,6-$Me_2C_6H_3$, R = C_6H_5
2c; R' = CMe_3, R = C_6H_5
2d; R' = 2,6-$Me_2C_6H_3$, R = CH_2CH_3

dissociation of the ligand to form the azametallacyclobutene (**2**). The alternative mechanism (Path B) involves reversible dissociation of the weakly bound ligand (L) to generate the coordinatively unsaturated transient imido complex (Cp_2Zr=NR), followed by reaction with an alkyne.

The observed rate constant (k_{obs}) for the associative reaction (path A) should be directly proportional to the concentration of the alkyne (eq 2). In the dissociative mechanism (Path B), however, one can predict that k_{obs} is not proportional to the concentration of the alkyne in the rate law

$$\text{Rate} = \frac{k_1 k_2 [RC{\equiv}CR][1]}{k_{-1} + k_2} = k_{obs}[1] \quad (k_{obs} \propto [RC{\equiv}CR]) \qquad (2)$$

(eq 3) calculated by applying the steady-state approximation to the reactive intermediate [Cp_2Zr=NR]. As k_2[alkyne] becomes much greater than k_{-1}[L] in the presence of high concentration of alkynes, k_{obs} will reach saturation and approach k_1, where no dependence of k_{obs} on the concentration of alkyne is observed. This mechanism also predicts that a reciprocal plot (eq 4) of $1/k_{obs}$ vs. [L]/[alkyne] should be linear.

$$\text{Rate} = \frac{k_1k_2[\text{alkyne}][1]}{k_2[\text{alkyne}] + k_{-1}[L]} = k_{obs}[1] \quad \left(k_{obs} = \frac{k_1k_2[\text{alkyne}]}{k_2[\text{alkyne}] + k_{-1}[L]}\right) \tag{3}$$

$$\frac{1}{k_{obs}} = \frac{1}{k_1} + \frac{k_{-1}}{k_1k_2} \times \frac{[L]}{[\text{alkyne}]} \tag{4}$$

The THF adduct $Cp_2Zr[N(2,6\text{-}Me_2C_6H_3)](THF)$ (**1a**) was first considered for the kinetic study. However, the cycloaddition rate of **1a** with alkynes was inconveniently rapid. It was determined by ^1H NMR spectroscopy that the formation of azametallacyclobutene in the reaction of alkyne with **1a** is complete in several seconds at -30 °C even in pure THF-d_8. Complexes analogous to **1a**, $Cp_2Zr[N(2,6\text{-}Me_2C_6H_3)](N\text{-}C_5H_4\text{-}p\text{-}CMe_3)$ (**1b**) and $Cp_2Zr[N(CMe_3)](OPPh_3)$ (**1c**), react more slowly with alkynes and were therefore more suitable for kinetic studies.

Kinetic Studies with 1b. It was decided to follow the rate of cycloaddition of diphenylacetylene with **1b** using UV/Vis spectroscopy by following the increase in the absorbance at 385 nm due to the formation of **2b.** To insure pseudo-first order conditions,[19] the initial concentration of diphenylacetylene used was at least 10 times that of **1b.** Under these conditions, the concentration of [diphenylacetylene]/[4-*tert*-butylpyridine] remained effectively constant during the reaction. Typical UV/Vis spectra for the formation of **2b** from **1b** in toluene at 50 °C are given in Figure 1. These show clear isosbestic points due to the existence of two species in equilibrium. Pseudo-first order rate constants ($k_{obs[1b]}$) obtained from the plots of $\ln(A_\infty - A_t)$ versus time to ≥ 3-half lives are also shown in Figure 1. The values of $k_{obs[1b]}$ for various concentrations of diphenylacetylene at each constant concentration of **1b** were obtained using same methods and are given in Table 1. The data show that the $k_{obs[1b]}$ values are dependent on (but not linearly) the ratio of [diphenylacetylene]/[*p*-tert-butylpyridine].

The plot of $k_{obs[1b]}$ versus the ratio of [diphenylacetylene]/[4-*tert*-butylpyridine] concentrations shown in Figure 2 exhibits saturation behavior. The reciprocal plot of $1/k_{obs[1b]}$ versus [4-*tert*-butylpyridine]/[diphenylacetylene] shows a straight line with a correlation coefficient of 0.985 (Figure 3). The data obtained from Figures 2 and 3 are consistent with a dissociative mechanism (Path B), in which a rapid pre-equilibrium involving the loss of 4-*tert*-butylpyridine is followed by the reaction with diphenylacetylene (Scheme I). The saturation and inverse plots (Figure 2 and 3) demonstrate that $k_{obs[1b]}$ eventually becomes equal to $k_{1[1b]}$ when $k_{2[1b]}$[diphenylacetylene] >> $k_{-1[1b]}$[4-*tert*-butylpyridine]. The value of $k_{1[1b]}$ can be obtained from the y-intercept of the plot in Figure 3; its value

Table 1. Rate constant (k_{obs}) data for the reaction of **1b** (1.98 ± 0.05M) with various concentration ratios of [diphenylacetylene]/[4-*tert*-butylpyridine].

[diphenylacetylene] x 10^4 (M)	[4-*tert*-butylpyridine] x 10^4 (M)	[diphenyacetylene]/ [4-*tert*-butylpyridine]	k_{obs} x 10^4 (sec^{-1})
23.79	12.90	1.84[a]	2.95 ± 0.07
35.68	12.90	2.77[a]	3.90 ± 0.10
23.79	6.45	3.69[a]	4.76 ± 0.12
78.30	20.00	3.92[b]	4.82 ± 0.12
35.68	6.45	5.53[a]	6.41 ± 0.16
35.70	6.45	5.54[a]	6.56 ± 0.16
47.58	6.45	7.38[a]	6.91 ± 0.17
156.60	20.00	7.83[b]	8.10 ± 0.20
59.47	6.45	9.22[a]	8.25 ± 0.21
71.36	6.45	11.06[a]	9.47 ± 0.24
83.26	6.45	12.91[a]	8.80 ± 0.22
95.15	6.25	14.75[a]	9.68 ± 0.24
313.20	20.00	15.66[b]	8.35 ± 0.21
626.40	20.00	31.32[b]	10.20 ± 0.26
1262.80	20.00	63.14[b]	14.59 ± 0.37
1517.60	20.00	75.88[b]	15.08 ± 0.38

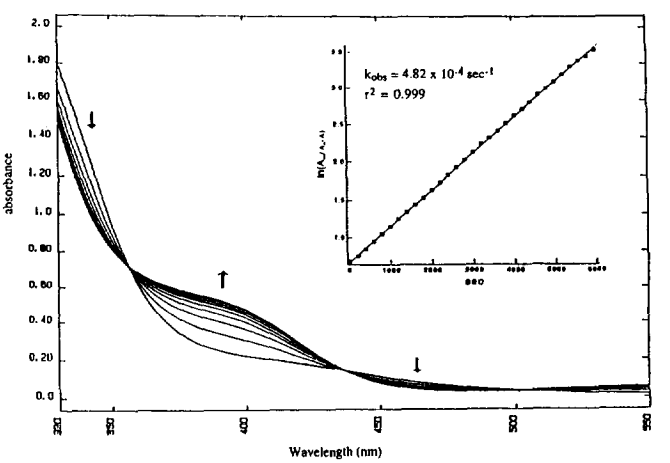

Figure 1. UV/Visible spectrum of the reaction of **1b** (1.95 x 10^{-4} M) with diphenylacetylene (35.68 x 10^{-4} M) in the presence of 4-*tert*-butylpyridine (6.45 x 10^{-4} M) in toluene at 50 °C and plot of ln (A_∞- A) versus time for the same reaction (inset). k_{obs} is 4.82 x 10^{-4} sec^{-1} and the linear fit gave a coefficient of r = 0.99.

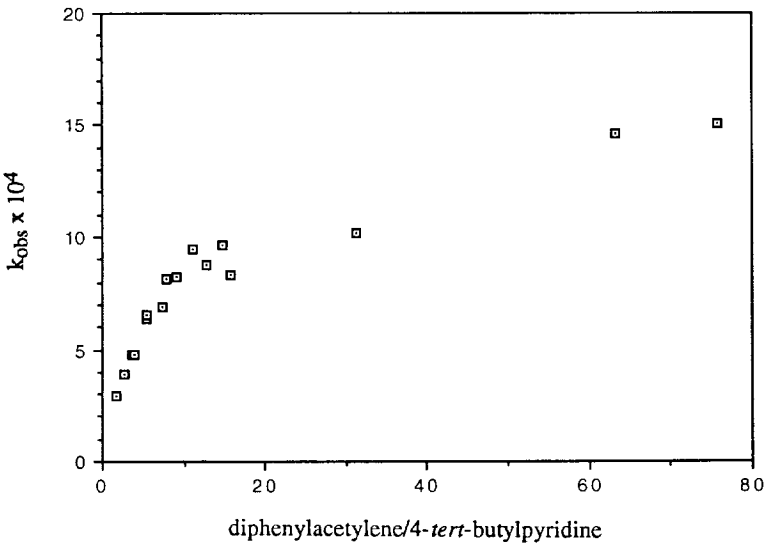

Figure 2. Plot of k_{obs} vs [diphenylacetylene]/[4-*tert*-butylpyridine].

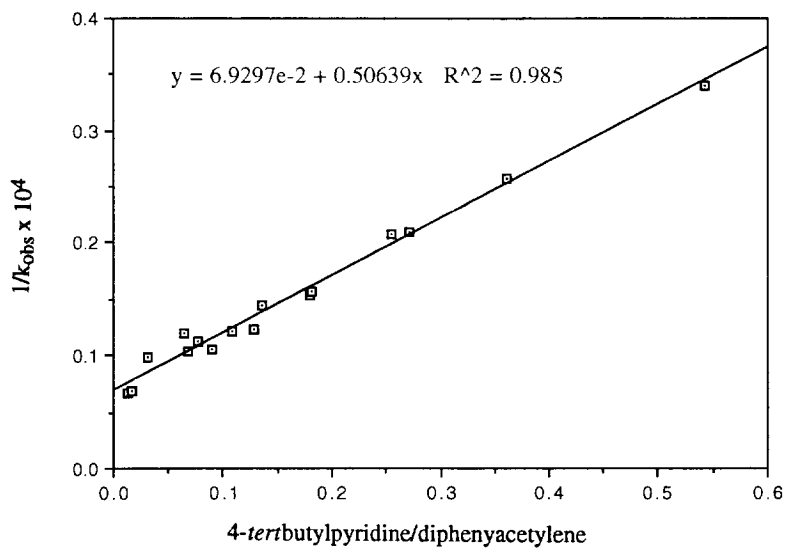

Figure 3. Plot of $1/k_{obs}$ vs [4-*tert*-butylpyridine]/[diphenylacetylene]. The linear fit gave a coefficient of $r = 0.99$.

is 1.44 x 10^{-3} sec^{-1} at 50 °C. The ratio of $k_{-1[1b]}/k_{2[1b]}$ can be calculated by multiplying the slope of the plot in Figure 3 by the value of k_1. This value, 7.29, shows that the imido intermediate reacts with 4-*tert*-butylpyridine 7.29 times faster than with diphenylacetylene at 50 °C.

Kinetic studies with 1c. The cycloaddition reaction of diphenylacetylene with the phosphine oxide complex **1c** at 50 °C was carried out under similar conditions. The increase in the absorbance at 391 nm due to formation of **2** was measured and $k_{obs[1c]}$ was calculated by plotting $\ln(A_\infty - A_t)$ versus time. Table 2 shows the value of $k_{obs[1c]}$ for a range of concentration ratios of [diphenylacetylene]/[PPh_3O]. A plot of $k_{obs[1c]}$ versus [diphenylacetylene]/[$OPPh_3$] (Figure 4) and the inverse plot of $1/k_{obs[1c]}$ vs. [PPh_3O]/[diphenyacetylene] (Figure 5) show that cycloaddition of the imido complex **1c** with diphenylacetylene once again follows the dissociative mechanism (Path B). Values of

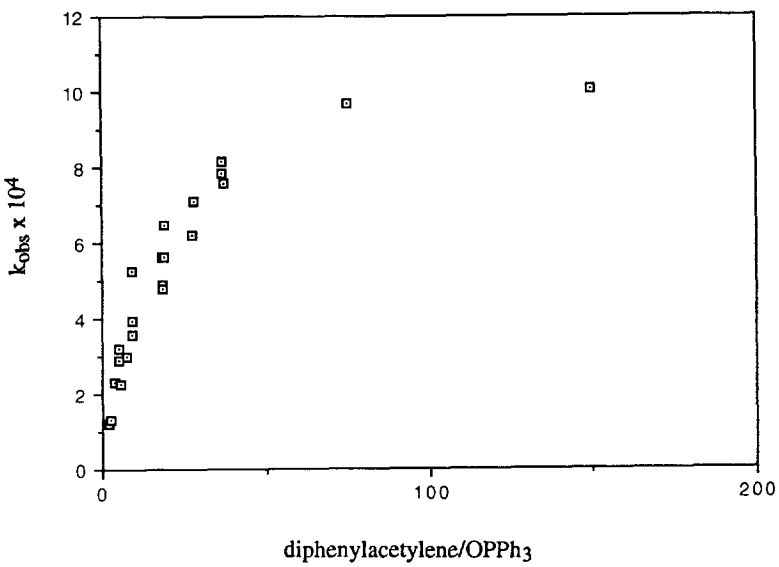

Figure 4. Plot of k_{obs} vs [diphenylacetylene]/[$OPPh_3$].

Table 2. Rate constant (k_{obs}) data for the reaction of **1c** with various concentration ratios of [di-p-tolylacetylene]/[$OPPh_3$] .

[diphenylacetylene] x 10^4 (M)	[$OPPh_3$] x 10^4 (M)	[diphenylacetylene] /[$OPPh_3$]	k_{obs} x 10^4 (sec^{-1})
4.40	2.80	1.57[a]	1.58 ± 0.14
8.58	4.51	1.90[a]	1.21 ± 0.11
41.97	17.96	2.34[b]	1.34 ± 0.12
17.16	4.51	3.81[a]	2.29 ± 0.21
41.97	8.98	4.67[b]	2.90 ± 0.26
21.99	4.49	4.90[b]	3.19 ± 0.29
25.74	4.51	5.71[a]	2.27 ± 0.20
34.32	4.51	7.61[a]	2.99 ± 0.27
41.58	4.51	9.22[a]	3.57 ± 0.32
41.58	4.51	9.22[a]	3.92 ± 0.35
41.97	4.49	9.35[b]	5.25 ± 0.47
83.16	4.51	18.44[a]	4.80 ± 0.43
83.16	4.51	18.44[a]	4.90 ± 0.44
83.16	4.51	18.44[a]	5.66 ± 0.51
83.94	4.49	18.70[b]	5.62 ± 0.51
84.94	4.51	18.83[a]	6.49 ± 0.58
124.70	4.51	27.65[a]	6.19 ± 0.56
125.91	4.51	27.92[a]	7.08 ± 0.64
166.30	4.51	36.87[a]	7.84 ± 0.71
166.32	4.51	36.88[a]	7.14 ± 0.64
84.00	2.24	37.50[b]	7.58 ± 0.68
168.00	2.24	75.00[b]	9.71 ± 0.83
335.79	2.24	149.91[b]	10.07 ± 0.91

[a] $[\mathbf{1c}]_o = 4.16 \times 10^{-4}$ M $[\mathbf{1c}]_o = 2.19 \times 10^{-4}$ M

Table 3. k_1 and k_{-1}/k_2 values obtained from the reaction of diphenylacetylene with **1b** and **1c**.

$Cp_2ZrNR(L)$	$Cp_2ZrN(2,6\text{-}Me_2C_6H_3)$(4-*tert*-pyridine) (**1b**)	$Cp_2ZrN(CMe_3)(OPPh_3)$ (**1c**)
k_1	1.44×10^{-3} sec^{-1}	1.02×10^{-3} sec^{-1}
k_{-1}/k_2	7.29	14.34

$k_{1[1c]}$ = 1.02 x 10^{-3} sec^{-1} and $k_{-1[1c]}/k_{2[1c]}$ = 14.34 derived from the inverse first-order plot in Figure 4 demonstrate that the imido intermediate reacts with $OPPh_3$ almost 14 times faster than with diphenylacetylene.

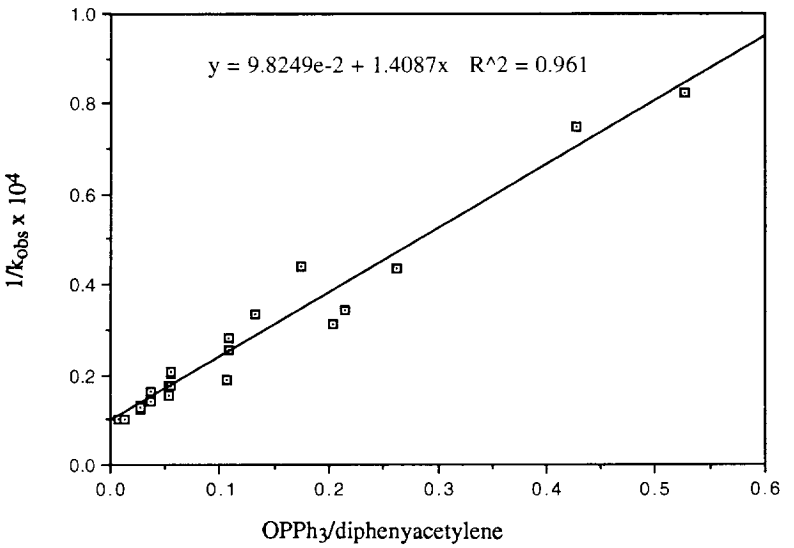

Figure 5. Plot of $1/k_{obs}$ vs [PPh_3O]/[diphenylacetylene]. The linear fit gave a coefficient of r = 0.96.

Competitive reaction of 1a with 3-hexyne and di-*p*-tolylacetylene. To investigate the selectivity of the intermediate for alkynes of different structure, the competitive cycloaddition reaction of di-*p*-tolylacetylene and 3-hexyne with the THF adduct **1a** was carried out (Scheme II). The reaction of

Scheme II

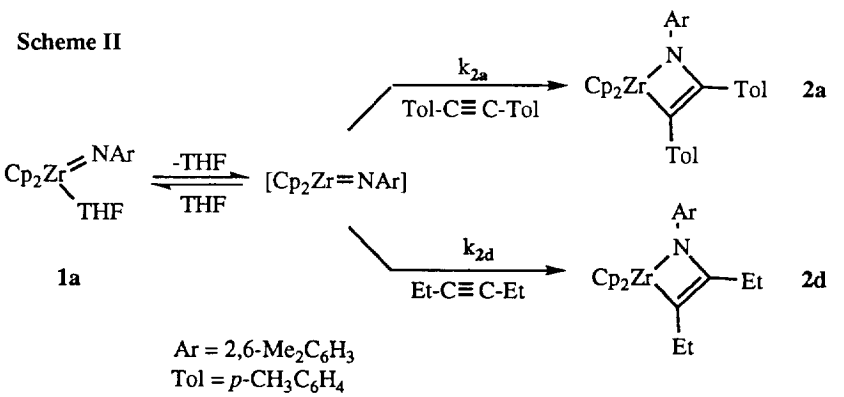

alkynes with **1a** to form azametallacyclobutenes is complete within seconds and is only very slowly reversible at RT.[5] Therefore, the cycloaddition reaction of **1a** with a tenfold excess of a mixture of the

two alkynes should yield the kinetically controlled mixture of metallacycles. If we assume the mechanism of this reaction is analogous to that determined for **1b** and **1c**, we can define the rate constant k_{2d} for the reaction with 3-hexyne and k_{2a} for the reaction of the intermediate $Cp_2Zr{=}NAr$ with di-*p*-tolylacetylene (Scheme II). The ratio of rate constants for the cycloaddition reactions is shown in eq 5.

$$\frac{k_{2a}}{k_{2d}} = \frac{[2a]_t}{[2d]_t} \times \frac{[3\text{-hexyne}]}{[\text{di-}p\text{-tolylacetylene}]} \tag{5}$$

Accurate concentrations of each alkyne were determined by integration of the one-pulse ^1H NMR spectrum of the reaction mixture, and the ratio of $[2a]_t/[2d]_t$ in eq 5 was obtained by measuring the ratio of the reaction products. From this calculation, the value of k_{2a}/k_{2d} was determined to be 0.75 ± 0.07 for a [3-hexyne]/[di-*p*-tolylacetylene] ratio of 0.75 ± 0.04 and 0.69 ± 0.04 for a [3-hexyne]/[di-*p*-tolylacetylene] ratio of 1.05 ± 0.02, respectively. These results show that k_{2a}/k_{2d} is not affected significantly by the ratio of alkynes and that the cycloaddition reaction of **1a** with 3-hexyne is kinetically more favorable than the reaction of **1a** with di-*p*-tolylacetylene at RT.

Table 4. k_{2a}/k_{3a} values with various concentration ratios of [3-hexyne]/[di-*p*-tolylacetylene].

[3-hexyne]/[di-*p*-tolylacetylene]	k_{2a}/k_{2d}
0.75 ± 0.04	0.75 ± 0.07
1.05 ± 0.02	0.69 ± 0.04

An attempt to determine the thermodynamically more stable cycloaddition adduct in this system by increasing the temperature to induce reversibility was unsuccessful because metallacycle **2d** reacted further with the excess of 3-hexyne introduced to obtain the kinetic product.[20] An alternate method of determining the thermodynamically stable metallacycle was based on equation 6. The azametallacyclobutene **2d** was separately synthesized by the reaction of **1a** with 3-hexyne at RT.

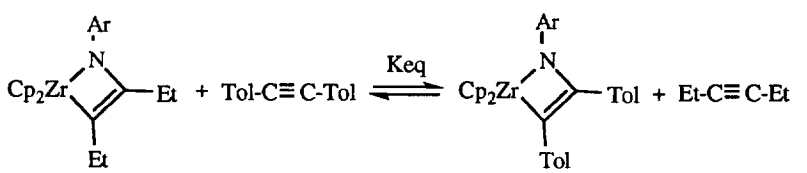

2d **2a** (6)

Recrystallized **2d** was then combined with 1 eq of di-*p*-tolylacetylene in C_6D_6. Under these conditions, the reaction of 3-hexyne with **2d** is very slow due to the low concentration of 3-hexyne.

At elevated temperature, **2d** and 1 eq of di-*p*-tolylacetylene equilibrate thermally to give a mixture of metallacycles **2d**, **2a** and the corresponding alkynes. This reaction presumably proceeds by initial extrusion of 3-hexyne from **2d** to form the intermediate $Cp_2Zr{=}NAr$ which then reacts with di-*p*-

tolylacetylene to form metallacycle **2a**. The amount of each compound in the equilibrium was measured by ^1H NMR integration against an internal standard. The equilibrium constant obtained for equation 6 is 15.7 ± 5.3 at 75 ± 1 °C and 16.8 ± 6.2 at 110 ± 2 °C. The equilibrium lies to the right at both temperatures, and has a slight tendency to move to the right with increased temperature.

Regiochemistry of 2+2 cycloaddition of electronically unsymmetrical diaryl alkynes with 1a. To investigate the electronic effect on the cycloaddition reaction, we studied the reaction of electronically unsymmetrical alkynes with **1a**. Several unsymmetrically *p*-substituted diphenylacetylenes ($XC_6H_4CCC_6H_4Y$; **3a** (X = H, Y = Cl); **3b** (X = CH_3, Y = H); **3c** (X=OCH_3, Y = H); **3d** (X = CH_3, Y = CF_3)) were synthesized by Stephens-Castro coupling[21] for this purpose and used for the cycloaddition reactions.

Scheme III

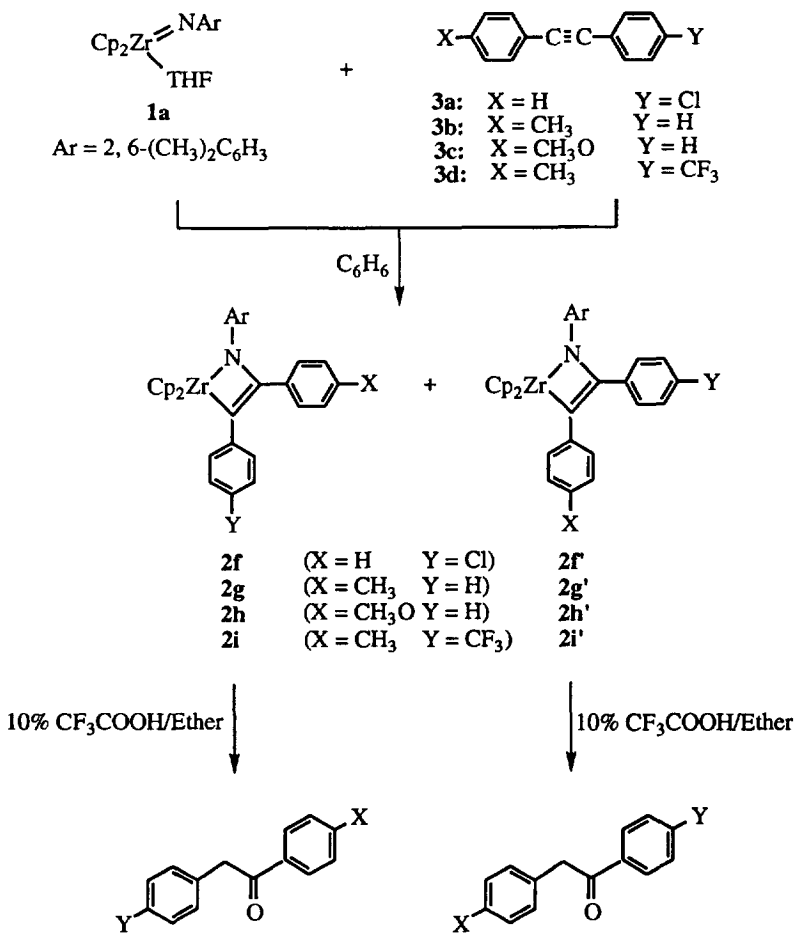

The reaction of **1a** with the para-substituted alkynes **3a-d** occurs within seconds at RT to give dark-green solutions of the product metallacycles **2** (Scheme III). Because mixtures of structurally very similar regioisomers are formed in each case, we did not try to separate and purify each individual isomer, but instead established the regiochemistry by hydrolysis and analysis of the resulting substituted deoxybenzoins (Scheme III; *ca.* 70% yields). The ratio of these ketones was measured by GC and GCMS. Yields of regioisomers formed at the elevated temperature were also obtained, in this case by integration of the one-pulse ^1H NMR spectrum of the reaction mixture against an internal standard. Table 5 shows the yields of regioisomers generated from the reaction of **3a-d** with **1a** at three different temperatures.

Table 5. The ratio of two regioisomers generated from the cycloaddition of **1a** with *p*-substituted diphenylacetylenes.

alkynes	Metallacycles	% by GC	% by NMR integration		
($XC_5H_4CCC_6H_4Y$)		RT	RT	68.5°C	100°C
3a	2f	39	40	57	58
(X = H, Y = Cl)	2f'	61	60	43	42
3b	2g	47	46	67	67
(X = CH_3, Y = H)	2g'	53	54	33	33
3c	2h	57	59	73	75
(X = OCH_3, Y = H)	2h'	43	41	26	26
3d	2i	32	35	82	dec.
(X = CH_3, Y = CF_3)	2i'	68	65	19	dec.

The ratios of regioisomers do differ somewhat from alkyne to alkyne, but the differences correspond to very small changes in $\Delta\Delta G^{\ddagger}$. Because of this we do not feel comfortable trying to interpret the changes that occur as the alkyne substituents vary. However, there is a discernible pattern in the regioisomers that predominate in the kinetic and thermodynamic product ratios. Considering first the isomer ratios obtained under reversible conditions at elevated temperatures (since the pattern seems somewhat clearer), the most thermodynamically stable metallacycles are those having the more electron withdrawing phenyl substituent located α to zirconium (**2f**, **2g**, **2h**, and **2i**). In contrast, the major isomers (**2f'**, **2g'**, and **2i'**) obtained under kinetic conditions at RT are those in which the more electron deficient aryl groups are located α to nitrogen, with one exception: the *p*-methoxy substituted metallacycle **2h**.

To look for a possible solvent effect on the regiochemistry of the cycloaddition, the reactions of *p*-substituted diphenylacetylenes were also examined in THF-d_8. The reaction of **3a** with **1a** in THF-d_8 at RT and 68.5 °C gave the same ratios of regioisomers within experimental error (± 5%) as the reaction in C_6D_6.

Regiochemistry of 2+2 cycloaddition of electronically unsymmetrical alkynes with 1e. The effect of changing the imido substituent was also studied. For this purpose, $Cp_2Zr{=}NCMe_3(THF)$ (**1e**), in which a *t*-Bu group is substituted for the 2,6-$(CH_3)_2C_6H_3$ group of **1a**, was chosen and the reaction of

Table 6. The ratio of two regioisomers generated from the cylcloaddition of **1e** with *p*-substituted diphenylacetylenes.

alkyne	Metallacycles	% by NMR integration			% by GC
$XC_5H_4CCC_6H_4Y$)		RT	68.5°C	100°C	100°C
3c	2j	51	68	68	67
(X = OCH_3, Y = H)	2j'	49	32	32	33
3d	2k	44	68	94	93
(X = CH_3, Y = CF_3)	2k'	56	32	6	7

1e with **3c** (or **3d**) in C_6D_6 was carried out. Table 6 shows the yields of the two metallacycles determined by integration of one pulse ^1H NMR spectra against an internal standard. Comparison of the results in Table 5 with those in Table 6 demonstrates that the regioselectivity of the cycloaddition is not significantly affected by this change. All values follow the same trends; **2j** and **2k** are favored at elevated temperature and **2k'** (but **2j** when **3c** was used for the reaction) is favored at RT.

Cycloaddition of *m*-$CH_3OC_6H_4CCC_6H_5$ (3e). In contrast to the reaction of other alkynes (**3a**, **3b**, and **3d**), the cycloaddition of **3c** with **1a** (and **1e**) produces the same major isomer **2h** (and **2j**) at both RT and the elevated temperature. In an attempt to understand these anomalous results, we examined the cycloaddition of *m*-$MeOC_6H_4CCC_6H_5$ (**3e**) with **1a** in C_6D_6 at RT and 100 °C. The overall electronic effect of **3e** was much smaller than that for **3c** (the ratio of regioisomers was 45:55 at RT and 52:48 at 100 °C).[22]

DISCUSSION

Kinetics of azametallacyclobutene formation: (a) with 1b. The kinetics of 2+2 cycloaddition of the imido complex **1b** with diphenylacetylene implicate a dissociative mechanism for the first step of the reaction. In the reaction of **1b** with various concentrations of diphenylacetylene (excess used to insure

pseudo-first-order kinetics), $k_{obs[1b]}$ is not linearly dependent on the concentration of alkyne. Instead, a plot of $k_{obs[1b]}$ versus the ratio of [diphenylacetylene]/[4-*tert*-butylpyridine] exhibits saturation kinetics, becoming zero order in [alkyne] at high alkyne/pyridine ratios. This requires that reaction involves a dissociative mechanism, proceeding through reversible formation of an intermediate which, at high alkyne concentrations, can be trapped more rapidly than it returns to starting imido complex (Path B in Scheme I). As predicted by this mechanism, a reciprocal plot of $1/k_{obs[1b]}$ versus [4-*tert*-butylpyridine]/[diphenylacetylene] is linear (Figure 3).

At saturation (i.e., when $k_{2[1b]}$[diphenylacetylene] >> $k_{-1[1b]}$[4-*tert*-butylpyridine]), $k_{obs[1b]}$ is equal to $k_{1[1b]} = 1.44 \times 10^{-3}$ sec^{-1} at 50 °C. We believe that the initial step associated with this saturation rate constant involves dissociation of the 4-*tert*-butylpyridine ligand to generate the transient imido complex $Cp_2Zr{=}NR$ or a solvate of this species. This intermediate then rapidly reacts with diphenylacetylene. The rate constant ratio $k_{-1[1b]}/k_{2[1b]}$ can be obtained from the inverse plot (Fig. 3; eq 4) by multiplying the slope by the reciprocal of the intercept. In this way we have determined that the imido intermediate $Cp_2Zr{=}N[2,6\text{-}(CH_3)_2C_6H_3]$ reacts with 4-*tert*-butylpyridine 7.29 times faster than with diphenylacetylene at 50 °C.

(b) with 1c. The cycloaddition reactions of diphenylacetylene with phosphine oxide complex **1c** demonstrate that changing the imido substituent and the dative ligand does not substantially affect the mechanism of the cycloaddition reaction. The plots in Figure 4 and 5 show that the reaction once again follows the dissociative mechanism (Path B). Values of $k_{1[1c]} = 1.02 \times 10^{-3}$ sec^{-1} and $k_{-1[1c]}/k_{2[1c]} = 14.3$ were derived from the inverse first-order plot in Figure 4.

Steric and electronic effects on azametallacyclobutene formation. Earlier studies in this group demonstrated that the regiochemistry of the cycloaddition reaction of sterically unsymmetrical alkynes with **1a** gives kinetically favored metallacycles in which the larger alkyne substituent is located α to the zirconium center, presumably due to steric repulsion between the N-substituent and the bulkier ligand on the alkyne (eq 7).[4,5] This effect increases with the size of the unsymmetrical alkyne, and in the case of

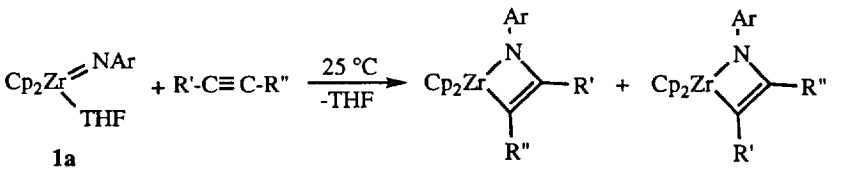

(7)

R' = CH_3, R" = Ph	82% (>99% at 110 °C)	18%
R' = CH_3, R" = *n*-Pr	86%	14%
R' = CH_3, R" = *i*-Pr	90%	10%
R' = CH_3, R" = *t*-Bu	>98%	-

$CH_3{\equiv}C$-*t*-Bu, only one regioisomer was observed. In this earlier system the kinetic and thermodynamic products ratios were nearly identical for the dialkylalkynes examined. However, in the case of $PhC{\equiv}CCH_3$, there was a larger amount of α-phenyl-substituted regioisomer in the thermodynamic than in the kinetic product. (eq 7).

It was hoped that further regiochemistry studies would help us to understand the factors controlling these product distributions. Therefore, as a first experiment the competitive cycloaddition reaction of **1a** with 3-hexyne and di-*p*-tolylacetylene was examined. The kinetic and thermodynamic selectivities are very different in this case: the dialkylacetylene cycloaddition product is favored kinetically, whereas the diarylacetylene product is favored thermodynamically. These results are consistent with the earlier study using sterically unsymmetrical alkynes. It appears that steric effects dominate the factors that control the relative energies of the cycloaddition transition states, whereas electronic factors (i.e., stabilization of the metallacycle by aryl substitution at the position α to the metal center) are more important in determining the relative ground state free energies of the cycloaddition products. It seems likely that electron-withdrawing aryl groups stabilize the partial negative charges on the vinylic carbon (and perhaps also on nitrogen) as shown below.

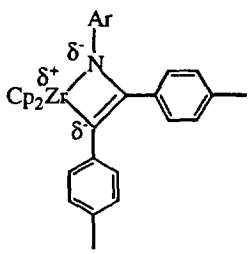

A more subtle question is whether there is any electronic control operating in the transition state in combination with the steric effects identified above. To answer this question, we have carried out the cycloaddition with electronically unsymmetrical, but sterically very symmetrical, alkynes. Unsymmetrically *p*-substituted diphenylacetylenes **3a-d** were chosen for this purpose. As mentioned earlier, the cycloaddition is fast and reversion of azametallacyclobutene to $Cp_2Zr{=}NR$ and alkyne is slow at RT.[5] We believe that the cycloadditions of **1a** with alkynes, therefore, are kinetically controlled at RT. In contrast, the cycloadditions at elevated temperatures are reversible and once again generate the thermodynamic ratio of regioisomers.

The results summarized in Table 5 and 6 identify overall electronic effects of *p*-substituents independent of competing steric effects for both the kinetic and thermodynamic product ratios. The overall conclusion is that the thermodynamic effects are modest in magnitude and reasonably comprehensible, but the kinetic effects are extremely small even in the reaction of **3d**, an alkyne possessing one donor and one acceptor substituent. In general the $\Delta\Delta G^{\ddagger}$ values leading to the two

isomers in each case (**2f**:**2f'**, **2g**:**2g'**, **2h**:**2h'**, or **2i**:**2i'**) are less than 1 kcal/mol. However, despite these weak electronic effects, there are analogies in the product patterns formed from most of the alkynes.

The thermodynamic effects seem to correlate well with our earlier regiochemical studies and therefore are the easier to understand. As before, the metallacycles with more electron-withdrawing substituents α to zirconium (**2f**, **2g**, **2h**, and **2i**) are thermodynamically favored. This supports our earlier conclusion that an electron-withdrawing group stabilizes partial negative charge on the benzylic carbon when it is located α to zirconium, and effectively rules out the possibility that the thermodynamic regiochemistry is controlled by some unusual steric effect in the examples cited above. The kinetic product ratios are more difficult to interpret. In contrast to the thermodynamic ratios, the kinetically favored isomers (**2f'**, **2g'**, and **2i'**) at RT are those in which the *less* electron deficient aryl groups are located α to zirconium, the one exception being the *p*-methoxy compound **2h**.

Ignoring **2h** for the moment, and keeping in mind that we are trying to interpret very small energetic effects, we conclude from these results is that the electronic factors that influence these transition state energy differences involve something other than the electron-withdrawing α–stabilizing effect observed in the azametallacycles. We suggest that the imido ligand is relatively basic and tends to associate with the more electropositive carbon of the alkyne, as illustrated in structure **A** below. Thus the (admittedly small) polarization in the transition state represented by **A** does not yet reflect the type of polarization in the final metallacycle products, as illustrated in **B**. The *p*-methoxy substituent is the strongest π–donor in the series, and we tentatively suggest that the unique kinetic regiochemistry

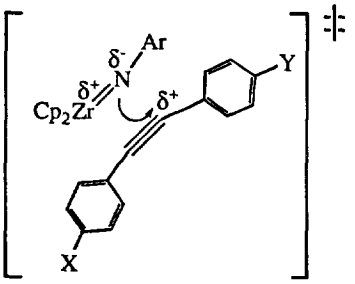

A

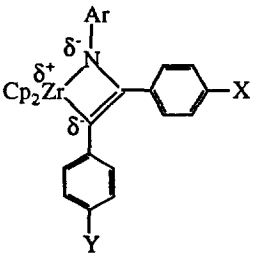

B

observed with (*p*-methoxyphenyl)(phenyl)acetylene may be due to this property of the substituent. The π–donating ability of the methoxy group tends to polarize the triple bond in such a way that the alkynyl carbon remote from the OMe group carries a slight negative charge, as shown in the drawing below. This could lead to a transition state in which this carbon is more readily attracted to the electropositive Zr center, resulting in the observed regiochemistry. Substituent effects on the energy of the product metallacycle, on the other hand, may involve the σ–bonding system more extensively and thus respond

more strongly to the (electron-withdrawing) inductive effect of the OMe group. Consistent with this idea, (*m*-methoxyphenyl)(phenyl)acetylene mimics both the kinetic and thermodynamic regiochemistry of the other alkynes, presumably because the OMe group can no longer "π–polarize" the triple bond in the transition state as shown above. We must emphasize, however, that the negligible effect on the regiochemistry caused by changing either the solvent (benzene vs. THF) or the N-substituent (2,6-dimethylphenyl vs. *tert*-butyl) suggest that any separation of charge that occurs in the transition state cannot be very large. This fact, and the very small energy differences revealed by the selectivity experiments, require great caution in attempts to interpret our results. We therefore offer the above explanation only as a working hypothesis rather than as a firm conclusion.

SUMMARY AND CONCLUSIONS

The kinetics of 2+2 cycloaddition of the imido complexes **1b** and **1c** with an internal alkyne (diphenylacetylene) are consistent with a dissociative mechanism (Path A in Scheme I), in which a rapid equilibrium involving loss of a dative ligand (**1b**: *t*-butylpyridine, **1c**: $OPPh_3$) generates an intermediate formulated as $Cp_2Zr{=}NR$ (R = 2,6-$(CH_3)_2C_6H_3$ for **1b**, CMe_3 for **1c**) or a solvate of this species. This initial step is followed by reaction of the intermediate with the alkyne. The reverse reaction of the imido intermediate with the dative ligand (L = $OPPh_3$ of **1b**, 4-*tert*-butylpyridine of **1c**) to form the starting imido complex (**1**) occurs more rapidly than reaction with diphenylacetylene to form the metallacycle (**2b** or **2c**) at 50 °C.

The competitive cycloaddition reactions of **1a** with 3-hexyne and di-*p*-tolylacetylene reveal that steric effects appear to be most important in controlling the relative stability of the cycloaddition transition state and electronic effects are somewhat more significant in the metallacycles. A study of the regiochemistry of the cycloaddition of unsymmetrically *p*-substituted diphenylacetylenes (**3a-d**) showed that the rates of formation of the metallacycles were affected only slightly by the electronic character of alkyne, although the modest magnitude of the effect makes it difficult to understand completely. At higher temperature, in the absence of large steric influences the thermodynamic stability of the metallacycles is determined by stabilization of a partial negative charge α to zirconium by electron withdrawing substituents. The negligible effect of changes in solvent or N-substituent on the regiochemistry supports a conclusion that the cycloaddition step proceeds via a four-center transition state having little charge separation.

EXPERIMENTAL

General. Unless otherwise noted, all reactions and manipulations were carried out under a nitrogen atmosphere at 25 °C in a Vacuum Atmospheres 553-2 dry box with a M6-40-1H Dritrain or by using standard Schlenk or vacuum line techniques. Degassed solutions were frozen to -196 °C, evacuated under high vacuum, and thawed. This sequence was repeated three times in each case. Glassware was dried at 150 °C before use. All ^1H NMR spectra were obtained on a 300- and 400 MHz Fourier Transform spectrometer at the University of California, Berkeley, NMR facility. The 300-MHz instruments were constructed by Mr. Rudi Nunlist and interfaced with either a Nicolet 1180 or 1280 computer. The 400-MHz instruments were commercial Bruker AM series spectrometers. ^1H NMR spectra were recorded relative to residual protiated solvent. $^{13}C\{1H\}$ NMR spectra were obtained at either 75.4 or 100.6 MHz on the 300- or 400-MHz instrument, respectively, and chemical shifts were recorded relative to the solvent resonance. Infrared spectra were recorded on a Nicolet 510 FTIR spectrometer. Elemental analyses were conducted by the University of California, Berkeley Microanalysis Facility. Sealed NMR tubes were prepared by using Wilmad 505-PP and 504-PP tubes attached via Cajon adapters directly to Kontes vacuum stopcocks and degassed using freeze-pump-thaw cycles before flame-sealing.[23]

Ultraviolet-visible (UV/Vis) spectra were recorded on a Hewlett Packard Model 8450 UV-Vis spectrometer in 1.00 cm quartz cells fused to Kontes Vacuum stopcocks. The temperature of the solutions during kinetic runs was maintained using a Hewlett Packard 89100A temperature controller. GC-MS spectra were obtained on a HP 5940 Series Mass Selective Detector attached to a Hewlett-Packard HP 5890A GC. Gas chromatography was performed with a Hewlett-Packard 5890A chromatography and HP-3396A integrator. A 30m capillary column containing 95:5 dimethylsilicone/methylphenylsilicone (DB-5) as the stationary phase and helium carrier gas was used for the separation. Preparative gas chromatography was carried out on a Varian 920 instrument using helium carrier gas. Standard columns were 3/8" stainless steel tubes packed with 10% OV-101 stationary phase on Chromsorb-WHP solid support. The injection port was lined with a 6 mm outer diameter glass tube.

Unless otherwise specified, all reagents were purchased from commercial suppliers. 2,6-Dimethylaniline and 4-*tert*-butylaniline were dried over sodium and distilled under vacuum. Pentane and hexanes(UV grade, alkene free) were distilled from sodium ketyl/tetraglyme under nitrogen. Benzene, toluene, ether, and THF were distilled from sodium benzophenone ketyl under nitrogen. Deuterated solvents for use in NMR experiments were dried as their protiated analogues and vacuum transferred from the drying agent. Compounds $Cp_2Zr(CH_2CH_2CMe_3)(Cl)$,[24] $Cp_2Zr(NH(2,6\text{-}Me_2C_6H_3))(CH_2CH_2CMe_3)$ (**3**),[25] $Cp_2Zr(THF)(N(2,6\text{-}Me_2C_6H_3))$ (**1a**),[4] $Cp_2Zr(OPPh_3)(NC_4Me_3)$ (**1c**),[4] and $Cp_2Zr(THF)(NC_4Me_3)$ (**1e**)[4] were prepared by literature methods. Triphenylphosphine oxide was obtained from Aldrich Chemical Co., recrystallized from absolute ethanol and dried in vacuum for 24 hrs before use. Reagent grade 3-hexyne was purchased from Farchan, dried over sodium under nitrogen, and vacuum transferred. Diphenylacetylene was obtained from Aldrich Chemical Co., dried over sodium in C_6H_6, and isolated by filtration and removal of benzene under reduced pressure. The *para*-substituted diphenylacetylenes ($XC_6H_4CCC_6H_4Y$; **3a** (X = H, Y = Cl); **3b** (X = CH_3, Y = H); **3c**

(X=OCH_3, Y = H); **3d** (X = CH_3, Y = CF_3)) were prepared by the interaction of copper(I) phenylacetylide with *para*-substituted iodobenzene.[21] They were purified until their melting points and IR spectral data agreed with published values[26] and their structures were confirmed by other spectral data (^1H NMR, ^{13}C NMR, and ^{19}F NMR). Azametallacyclobutenes $C_{34}H_{33}NZr$ (**2a**), $C_{32}H_{29}NZr$ (**2b**), and $C_{28}H_{29}NZr$ (**2c**) are reported elsewhere.[5] Compound **2d** was prepared by the reaction of **1a** and 3-hexyne according to the procedure of Baranger and Bergman.[27]

$Cp_2Zr(N(2,6\text{-}Me_2C_6H_3))(NC_5H_4(4\text{-}CMe_3))$ (1b). A glass bomb was loaded with $Cp_2Zr(NH(2,6\text{-}Me_2C_6H_3))(CH_2CH_2CMe_3)$ (**3**)[25] (345 mg, 8.09 x 10^{-1} mmol), *p-tert*-butylpyridine (547 mg, 405 mmol) and 10 mL benzene. The solution was degassed by two freeze-pump-thaw cycles and heated to 105 °C for 48 h, and then the solvent was removed subsequently under reduced pressure, providing an orange solid. Extraction into 4 mL of toluene, layering the solution with 6 mL hexane and cooling to -30 °C gave reddish orange crystals. Filtration provided 167 mg (44 % yield) of **1b**. ^1H NMR (400 MHz, C_6D_6): 8.52 (m, 2H, $NC_2\mathit{H}_2C_2H_2CCMe_3$), 7.27 (d, *J* = 7.35 Hz, 2H, Ar-*H*), 6.75 (t, J = 7.31 Hz, 1H, Ar-*H*), 6.60 (m, 2H, $NC_2H_2C_2\mathit{H}_2CCMe_3$), 6.01 (s, 10H, $C_5\mathit{H}_5$), 2.41 (s, 6H, 2,6-$(C\mathit{H}_3)_2$-Ar), 0.87 (s, 9H, $NC_5H_4C(C\mathit{H}_3)_3$). $^{13}C\{^1H\}$ NMR (400 MHz, C_6D_6): d(C) 164.0, 159.9, 125.5, 34.7; d(CH) 153.7, 128.1, 121.1, 115.1, 110.8; d(CH_3) 21.3, 29.8. IR (C_6H_6) 1300 (s), 1314 (s), 1405 (s), 1436 (w), 1448 (w), 1457 (m), 2968 (w) cm^{-1}; Anal. Calcd for $C_{27}H_{32}N_2Zr$ (**1b**): C, 68.16; N, 5.89; H, 6.78. Found: C, 68.36; N, 5.58; H, 6.74.

UV Kinetic Studies with $Cp_2Zr(N(2,6\text{-}Me_2C_6H_3))(NC_5H_4(4\text{-}CMe_3))$ (1b). UV/Vis spectroscopy was used to study the kinetics of the formation of azametallacyclobutene **2b** from diphenylacetylene and **1b**. Comparison of the UV/Vis spectra of **1b** and **2b** in toluene showed a very small region (330 to 480 nm) in which there was a significant difference in the absorbance between the two species .

The following stock solutions were prepared in toluene: diphenylacetylene, 5.95 x 10^{-3} M, 1.89 x 10^{-2} M; 4-*tert*-butylpyridine, 6.45 x 10^{-3} M; **1b**, 1.95 x 10^{-3} M. These solutions were stored in the dry box at -30°C. The reactions were performed under pseudo-first order conditions using at least 10 eq of diphenylacetylene. The initial concentration of **2** was held constant at 1.95 x 10^{-3} M for each run and the concentrations of diphenylacetylene and 4-tert-butylpyridine were varied. The reaction rate was monitored by following the increase in absorbance at 385 nm due to the formation of azametallacyclobutene. The transfer of stock solutions was accomplished using volumetric pipets. The interval between measurements was generally 400 s, but this was increased for slower runs and decreased for faster runs. The reaction was followed for at least 3 half-lives.

The procedure used for a typical run follows: A 10 mL volumetric flask was charged with 1.0 mL of 1.95 x 10^{-3} M solution of **1b**, 3 mL of 1.89 x 10^{-2} M solution of diphenylacetylene, and 1 mL of 6.45 x 10^{-3} M solution of *p*-tert-butylpyridine. The solution was then diluted to 10.0 mL using toluene and mixed by inverting the stoppered flask several times. A 1.00 cm quartz cell sealed to a Kontes vacuum stopcock was filled with the solution, stoppered in the dry box and quickly placed in the temperature

controller. It was allowed to equilibrate for 3 minutes before measurements were taken. After the reaction had progressed for at least 3 half-lives, measurements were terminated.

The change in absorbance versus time was plotted and the infinity point (A_∞) was calculated using a least squares program written in house in turbo Pascal which fit the increasing exponential to the equation: Abs = A_1*(1-Exp(-A_2*t)) + A_3; where the sum of A_1 and A_3 is equal to A_∞. Plots of ln(A_∞ - A_t) versus time were made and the observed rate constant was calculated from the slope using a linear least squares program. These plots were linear ($r^2 > 0.999$) for at least 3 half lives. To ascertain the reproducibility of the results, runs which should have the same k_{obs} were conducted not only at the same concentrations of diphenylacetylene and *p*-tert-butylpyridine but also at various concentrations with the same ratio of [diphenylacetylene]/[*p*-tert-butylpyridine] (Table 1). The measurements in the different concentration of **1b** (2.02×10^{-4} M) were also carried out. From these runs, we estimate an error limit of ± 2.5%.

UV kinetic studies using $Cp_2Zr(NCMe_3)(OPPh_3)$ (1c). The above UV/Vis techniques were used to study the kinetics of the formation of $Cp_2Zr[N(2,6\text{-}Me_2C_6H_3)][C_2(C_6H_5)_2]$ (**2c**) in the reaction of di-*p*-tolylacetylene and **1c**. The following stock solutions were prepared for the experiments: di-*p*-tolylacetylene, 1.36×10^{-2} M, 4.16×10^{-2} M; $OPPh_3$, 4.20×10^{-3} M; **1c**, 4.16×10^{-3} M. Using the same method as for the reaction of **1b** with diphenylacetylene, the sample solution was prepared, transferred to the 1.0 cm quartz UV cell sealed to Kontes vacuum stopcock, monitored by following the increase in absorbance at 390 nm for at least 3 half-lives, and plotted. These plots were used to determine the rate constants k_{obs} with an estimated error limit of ± 9% (Table 2).

Competitive azametallacyclobutene formation from 1a. ^{1}H NMR spectrometry was used to study the formation of azametallacyclobutenes from **1a**, 3-hexyne and di-*p*-tolylacetylene. An NMR tube was charged with di-*p*-tolylacetylene (20 mg, 9.7×10^{-2} mmol), 3-hexyne (6.0 mg, 7.3×10^{-2} mmol, 7.5 eq for the first trial; 8.5 mg, 10.2×10^{-2} mmol, 10.7 eq for the second trial), and 1.0 mL C_6D_6. The initial concentration of volatile 3-hexyne was determined by integration of the ^{1}H NMR spectrum against di-*p*-tolylacetylene. Immediately after integrating the amount of each alkyne in 0.5 mL C_6D_6 in a capped NMR tube, THF adduct **1a** (4.0 mg, 9.7×10^{-3} mmol) and 0.5 mL C_6D_6 were added to the solution in the NMR tube in the dry box. The solution was mixed by shaking the NMR tube several times; it turned dark red within seconds. The solution was degassed by two freeze-pump-thaw cycles and the NMR tube was flame sealed. Following equilibration in the NMR probe for 3 min a one-pulse ^{1}H NMR spectrum was taken. After 3 min another one pulse ^{1}H NMR spectrum was taken. Scans were exponentially multiplied, Fourier transformed and plotted with integrals. The ratio of each azametallacyclobutene (**2a** and **2d**) was determined by integration of the cyclopentadienyl peak against the internal standard. The integration was measured for each one-pulse ^{1}H NMR spectrum and then the results from the two spectra were averaged. The concentrations of the remaining unreacted alkynes were also determined by integration of each ^{1}H NMR spectrum.

Equilibration of azametallacyclobutenes. An NMR tube was charged with **3a** (14 mg, 2.5 x 10^{-2} mmol), di-*p*-tolylacetylene (54 mg, 2.5 x 10^{-2} mmol), *p*-dimethoxybenzene (3.5 mg, 2.5 x 10^{-2} mmol), and 0.7 mL of C_6D_6. The solution was degassed and the NMR tube was flame sealed. Immediately after mixing the solution, the initial concentration of each compound in the NMR tube was measured by integration against *p*-dimethoxybenzene for each one-pulse ^1H NMR spectrum at 25 °C. After confirming that formation of **2a** did not occur at 25 °C, the sample was heated to 75 °C for 8.3 h and cooled to 25 °C. The ratio of the thermodynamic products, **2a** and **2d**, was then measured by integration against *p*-dimethoxybenzene. Heating the sample for another 24 hrs at 75 °C did not change the ratio of products (**2a** and **2d**) within the experimental error limits of the ^1H NMR measurements (5%). The sample was then heated to 110 °C for 4 d. The ratio of **2a**:**2d** was determined by integration against *p*-dimethoxybenzene. The equilibrium constant K_{eq} at 110 °C was calculated using these data. To avoid the error from the change of the ratio of the equilibrium products in 75 °C and 110 °C, the reaction tube was quenched rapidly before each measurement.

Regiochemistry and determination of unsymmetric azametallacyclobutenes. (a) By ^1H NMR. An NMR tube was charged with **1a** (*ca.* 3 x 10^{-2} mmol), *p*-substituted diphenylacetylene (3-4 eq compared to **1a**), *p*-methoxybenzene (*t*-butylbenzene when **3c** was used), and 0.7 mL of C_6D_6. Immediately after mixing the solution, the kinetic ratio of regioisomers at RT was measured by integration against *p*-dimethoxybenzene for each one-pulse ^1H NMR spectrum. For the thermodynamic reaction, the NMR tube was degassed and the tube flame-sealed, heated to 68.5 °C for 1d, and quickly cooled to 25 °C. The ratio of the thermodynamic products, **2f-i** and **2f'-i'**, was measured until no change of the ratio between regioisomers at 68.5 °C was observed. The sample was then heated to 100 °C for 1d, cooled quickly to 25 °C, and the ratio of **2f-i**:**2f'-i'** was determined by integration against *p*-dimethoxybenzene. **(b) By GC and GCMS.** Under an inert atmosphere, the NMR tube was opened, and the volatile materials were removed under vacuum, leaving a purple solid. This solid was dissolved in 1 mL of diethyl ether, and in air, 0.5 mL of 10% CF_3COOH was immediately added; the solution was then shaken until both layers were clear. The ether layer was taken by pipet, neutralize with saturated $NaHCO_3$ solution, and analyzed by GC and GCMS. The ratio of corresponding substituted deoxybenzoins was determined by integration of the GC trace corrected for differences in response factors by calibration of the GC integrator using a cyclohexanone standard. The overall yields of hydrolysis of metallacycles was determined by integration of GC peaks against the known amount of benzoin added into the ether solution before the hydrolysis (*ca.* 70% yields).

ACKNOWLEDGMENTS

We acknowledge the National Institutes of Health (Grant No. R37-GM25459) for generous financial support of this work.

REFERENCES AND NOTES

(1) Nugent, W. A.; Mayer, J. M. *Metal Ligand Multiple Bonds*; Wiley: New York, 1988.

(2) Nugent, W. A.; Haymore, B. L. *Coord. Chem. Rev.* **1980**, *31*, 123.

(3) Walsh, P. J.; Hollander, F. J.; Bergman, R. G. *J. Am. Chem. Soc.* **1988**, *110*, 8730.

(4) Walsh, P. J.; Hollander, F. J.; Bergman, R. G. *Organometallics* **1993**, *12*, 3705.

(5) Walsh, P. J.; Baranger, A. M.; Bergman, R. G. *J. Am. Chem. Soc.* **1992**, *114*, 1708.

(6) Baranger, A. M.; Walsh, P. J.; Bergman, R. G. *J. Am. Chem. Soc.* **1993**, *115*, 2753.

(7) Meyer, K. E.; Walsh, P. J.; Bergman, R. G. *J. Am. Chem. Soc.* **1994**, *116*, 2669.

(8) Bennett, J. L.; Wolczanski, P. T. *J. Am. Chem. Soc.* **1994**, *116*, 2179.

(9) McGrane, P., L.; Jensen, M.; Livinghouse, T. *J. Am. Chem. Soc.* **1992**, *114*, 5459.

(10) McGrane, P. L.; Livinghouse, T. *J. Org. Chem.* **1992**, *57*, 1323.

(11) de With, J.; Horton, A. D. *Organometallics* **1993**, *12*, 1493.

(12) Brown-Wensley, K. A.; Buchwald, S. L.; Cannizzo, L.; Clawson, L.; Ho, S.; Meinhardt, D.; Stille, J. R.; Straus, D.; Grubbs, R. H. *Pure. Appl. Chem* **1983**, *55*, 1733.

(13) Wood, C. D.; McLain, S. J.; Schrock, R. R. *J. Am. Chem. Soc.* **1979**, *101*, 3210.

(14) Mayr, A.; Lee, K. S.; Kjelsberg, M. A.; Van Engen, D. J. *1986* **1986**, *108*, 6079.

(15) Masuda, T.; Susaki, N.; Higashimura, T. *Macromolecules* **1975**, *8*, 717.

(16) Katz, T. J.; Hacker, S. M.; Kendrick, R. D.; Yannoni, C. S. *J. Am. Chem. Soc.* **1985**, *107*, 2182.

(17) Strutz, H.; Dewan, J. C.; Schrock, R. R. *J. Am. Chem. Soc.* **1985**, *107*, 5999.

(18) Ivin, K. J.; Rooney, J. J.; Stewart, C. D.; Green, M. L. H. *J. Chem. Soc. Chem. Comm.* **1978**, 604.

(19) Espenson, J. H. *Chemical Kinetics and Reaction Mechanisms*; McGraw-Hill: New York, 1981, pp 112.

(20) The cycloaddition reaction of **1a** with a tenfold excess of 3-hexyne at elevated temperature gradually generates a product tentatively assigned as an azametallacyclohexadiene by double insertion of 3-hexyne. The characterization of this doubly inserted product was not successful due to its instability. This double insertion does not occur in the reaction of the more sterically hindered di-p-tolylacetylene.

(21) Stephens, R. D.; Castro, C. E. *J. Org. Chem.* **1963**, *28*, 3313.

(22) The identification of the two regioisomers was not successful because the GC retention times of the corresponding benzoins were too similar to allow resolution of the two peaks.

(23) Bergman, R. G.; Buchanan, J. M.; McGhee, W. D.; Periana, R. A.; Seidler, P. F.; Trost, M. K.; Wensel, T. T. In *Experimental Organometallic Chemistry: A practicum in Synthesis and Characterization*; Wayda, A. L.; Darensbourg, M. Y. Eds; ACS Symposium Series 357; American Chemical Society: Washington, DC, 1987; p227.

(24) (a) Hart, D. W.; Schwartz, J. J. *J. Am. Chem. Soc.* **1974**, *96*, 8115. (b) Bertelo, C. A.; Schwartz, J. *J. Am. Chem. Soc.* **1975**, *97*, 228. (c) Labinger, J. A. Hart, D. W.; Seibert, W. E., III; Schwartz, J. *J. Am. Chem. Soc.* **1975**, *97*, 3851. (d) Bertelo, C. A.; Schwartz, J. *J. Am. Chem. Soc.* **1976**, *98*, 262.

(25) Baranger, A. M.; Walsh, P. J.; G., B. R. *J. Am. Chem. Soc.* **1993**, *115*, 2753.

(26) Eisch, J. J.; Hordis, C. K. **1971**, *93*, 2974 and references therein.

(27) Baranger, A. M. *Ph. D. Thesis*; University of California, Berkeley: 1994.

(*Received* 28 *October* 1994)